Magnetic field driven 2D-3D crossover in the $S = \frac{1}{2}$ frustrated chain magnet $LiCuVO_4$

L. A. Prozorova,[1] S. S. Sosin,[1,*] L. E. Svistov,[1,†] N. Büttgen,[2] J. B. Kemper,[3] A. P. Reyes,[3] S. Riggs,[3] A. Prokofiev,[4] and O. A. Petrenko[5]

[1]*P.L. Kapitza Institute for Physical Problems RAS, 119334 Moscow, Russia*

[2]*Center for Electronic Correlations and Magnetism (EKM), Experimentalphysik V, Universität Augsburg, D-86135 Augsburg, Germany*

[3]*National High Magnetic Field Laboratory, Tallahassee, Florida 32310, USA*

[4]*Institut für Festkörperphysik Technische Universität Wien, A-1040 Wien, Austria*

[5]*Department of Physics, University of Warwick, Coventry CV4 7AL, United Kingdom*

(Received 13 January 2015; revised manuscript received 14 April 2015; published 11 May 2015)

We report on a heat-capacity study of high-quality single-crystal samples of $LiCuVO_4$—a frustrated spin $S = \frac{1}{2}$ chain system—in a magnetic field amounting to 3/4 of the saturation field. A detailed examination of magnetic phase transitions observed in this field range shows that although the low-field helical state clearly has three-dimensional properties, the field-induced spin-modulated phase turns out to be quasi-two-dimensional. The model proposed in this paper allows one to qualitatively understand this crossover, thus eliminating the presently existing contradictions in the interpretations of NMR and neutron-scattering measurements.

DOI: 10.1103/PhysRevB.91.174410 PACS number(s): 75.10.Pq, 75.10.Jm, 75.50.Ee, 76.60.−k

I. INTRODUCTION

Quantum-spin chains with frustrated exchange interactions were among the most interesting issues for both experimental and theoretical research in condensed-matter physics of the past decade [1–3]. The enhanced effect of quantum fluctuations imposed upon a fine balance of exchange interactions leads to a variety of novel ground states and phase transformations in these systems [4–7]. $LiCuVO_4$ is an example of a quasi-one-dimensional (1D) magnet whose unconventional magnetic phases result from a competition of ferromagnetic and antiferromagnetic exchange interactions between nearest-neighbor (J_1) and next-nearest-neighbor (J_2) in-chain spins. As a result of this particular combination of exchange interactions a helical incommensurate spin structure is stabilized in this system below $T_N \approx 2.3$ K [8]. A strong reduction in the ordered spin component of Cu^{2+} ions in this state $\langle\mu\rangle/\mu_B \simeq 0.3$ (Refs. [8,9]) provides evidence that the system partially retains properties of 1D chains.

Moderate applied magnetic fields of 7 to 8 T induce a transformation of the spin helix into a collinear spin-modulated (SM) structure in which all the spins are parallel to the field with their ordered components oscillating along the chain with an incommensurate period. This transition may be related to the field evolution of short-range chiral (transverse) and spin-density wave (longitudinal) correlations for the 1D J_1-J_2 model [10].

In the field range just below the saturation field ($\mu_0 H_{\rm sat} \simeq$ 45 T) (Ref. [11]) the theory predicts the presence of a long-range nematic ordering [7,12]. The magnetic properties of $LiCuVO_4$ in this field range were studied by pulse magnetization and nuclear magnetic resonance (NMR) techniques [11,13]. These experiments determined the field range where the spin nematic phase can exist.

The present paper focuses on a specific heat study of the magnetic transitions into the helical and SM ordered phases. The helical state occurs at low fields up to about 7 T via a sharp λ anomaly in the specific heat curves followed by $C_p \propto T^3$ three-dimensional (3D) behavior at lower temperatures. The transition into a SM phase at higher fields is accompanied by a humplike anomaly which, as the temperature decreases further turns into a $C_p \propto T^2$ law distinctive for a quasi-two-dimensional (2D) system. We suggest an explanation for how nonmagnetic defects in the Cu^{2+} chains can suppress 3D long-range ordering in the SM phase and leave it undisturbed in the helical phase. This model eliminates the existing discrepancy in interpretations of NMR (Refs. [13–15]) and neutron-scattering measurements [16]. It also provides clear experimental evidence that further analysis of the phase diagram of $LiCuVO_4$ in the vicinity of the saturation field is required.

II. EXPERIMENTAL RESULTS

Single crystals of $LiCuVO_4$ grown by the methods described in Ref. [17] belong to the same series as the ones studied in our previous high-field NMR experiments [13]. The main part of the specific heat measurements were carried out in the Tallahassee National High Magnetic Field Laboratory with the use of a homemade relaxation-type calorimeter operating at temperatures 1.8–30 K in magnetic fields up to 35 T. Supplementary measurements were performed on a Quantum Design Physical Property Measurement System (PPMS) with a ^{3}He insert and a 9-T cryomagnet. The samples of 0.67 and 5.8 mg by mass were studied in the first and the second experiments, respectively. The magnetic field was applied along the c axis of the crystal.

Zero-field results obtained in both experiments and presented in Fig. 1 are in perfect agreement with each other. The phonon contribution to the heat capacity (expressed in units of J K^{-1} mol^{-1}) has been approximated by the function $C_p = 1.4 \times 10^{-4} T^3$ (the solid line in the upper panel). It was chosen so that the magnetic entropy (with the phonon part subtracted) attains the value of $0.7R\ln 2$ at a temperature of 30 K in agreement with numerical results for the 1D J_1-J_2 model [18]. This rough estimation gives a correction to the

*sosin@kapitza.ras.ru
†svistov@kapitza.ras.ru

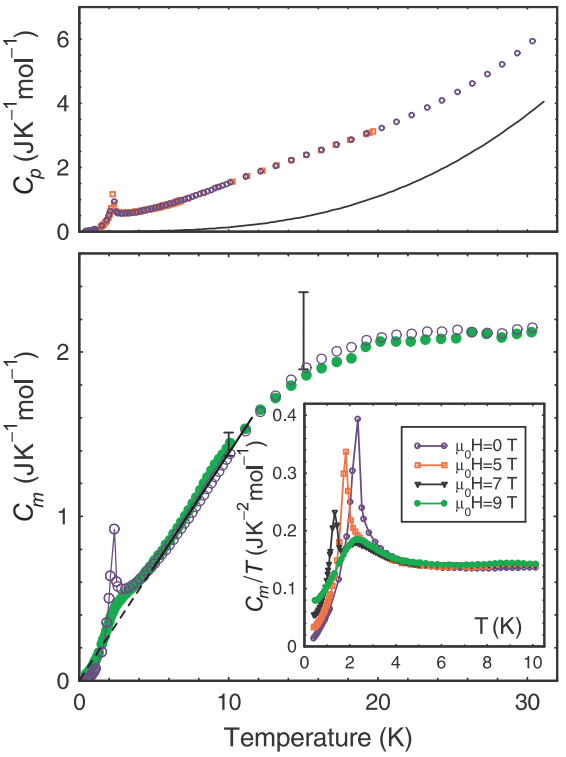

FIG. 1. (Color online) Upper panel: temperature dependence of the specific heat at zero magnetic field measured using a PPMS (circles) and using a homemade high-field setup (squares); the solid line is an approximation of the phonon contribution to the heat capacity. Lower panel: magnetic specific heat $C_m(T)$ (phonon contribution subtracted) of the sample measured in a PPMS at $\mu_0 H = 0$ (○) and 9 T (●), the error bars are explained in the text, and the solid line is a linear fit to both curves in the temperature range from 5 to 10 K; the inset shows the specific heat divided by temperature as a function of T obtained at several values of magnetic field (see the legend).

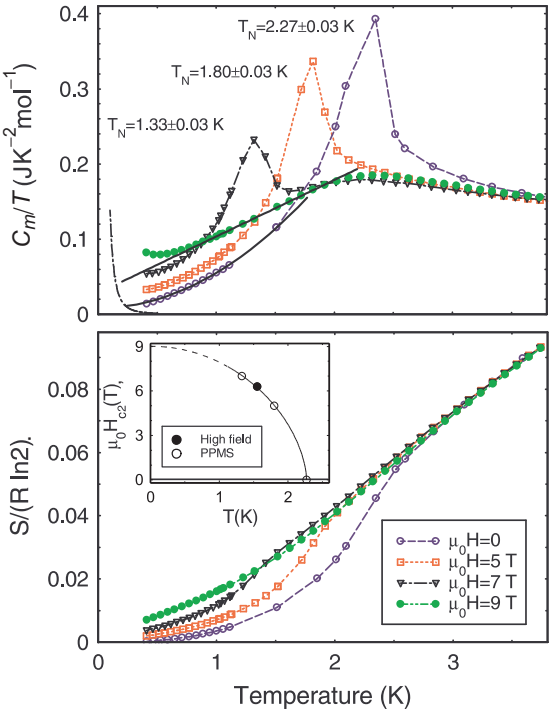

FIG. 2. (Color online) Upper panel: Expansion of the low-temperature part of the inset to Fig. 1, solid lines are quadratic and linear extrapolations to the zero field and 9 T curves, respectively, and the dashed-dotted line is a calculated contribution from ^{63}Cu and ^{65}Cu nuclei at the field 10 T. Lower panel: integrated $C_m/T(T)$ curves at various field values normalized to Rln2; the inset shows the boundary of the helical state obtained from both the PPMS and the high-field measurements (conforming with the previous study Ref. [21]), and the line is a guide to the eye.

total heat capacity of about 3%, 8%, and 20% at $T = 5$, 10, and 15 K, respectively, shown by the error bars in the lower panel of Fig. 1. Within these bounds our data conform with previous measurements [19,20]. This panel shows a comparison between the magnetic part of the specific heat $C_m(T)$ obtained at zero field and at a field of 9 T in the PPMS measurements. No significant difference between the two curves is observed in the high-temperature range. All the data in the lower panel of Fig. 1 exhibit temperature dependences $C_m \propto T$ in the range of 5–10 K providing evidence for the presence of 1D short-range correlations in the spin chains. The linear in temperature section of a zero-field curve is followed by a sharp λ anomaly at the transition into a 3D helical phase at $T_N = (2.27 \pm 0.03)$ K in agreement with a number of previous studies [8,9]. The inset to the lower panel of Fig. 1 presenting $C_m/T(T)$ curves at various fields traces the evolution of this transition shifting to low temperatures as the field increases. For the field $\mu_0 H = 9$ T which is greater than the field of the transition into a SM phase a λ anomaly is replaced by a humplike feature followed by a $C_m \propto T^2$ dependence towards lower temperatures. This curve slightly deviates from the square law at lowest temperatures.

This low-temperature part of the data requires more careful investigation and is expanded in the upper panel of Fig. 2. The phase transition at zero field is followed by a distinct $C_m \propto T^3$ behavior of the specific heat with a small linear contribution revealing itself at the lowest temperature (the corresponding fit is presented in Fig. 2). Shifting of the Néel temperature under magnetic field (T_N values are annotated in the upper panel and shown by open circles in the inset to the lower panel) is accompanied by the increase in this low-T contribution. In the absence of the transition peak at $\mu_0 H = 9$ T the high-T linear part of the curve is converted into a quasi-2D $C_m \propto T^2$ law extending for half a decade by temperature (see linear fit to the C_m/T curve for 9 T). The low-T rise of this curve might indicate the proximity to a 3D transition. Extrapolation of the phase boundary $\mu_0 H_{c2}(T_N)$ (see the inset to the lower panel of Fig. 2) to zero temperature gives the value $\mu_0 H_{c2}(0) \simeq 9$ T. Alternatively, this rise could be attributed to the specific heat of the Cu nuclei (the corresponding curve estimated for the external field 10 T and zero hyperfine field is shown in Fig. 2). In any case, the total entropy evolved in the process of low-T disordering does not depend on the external field in this field range: The corresponding functions obtained by integration of $C_m/T(T)$ curves converge at temperatures above the ordering transition at zero field.

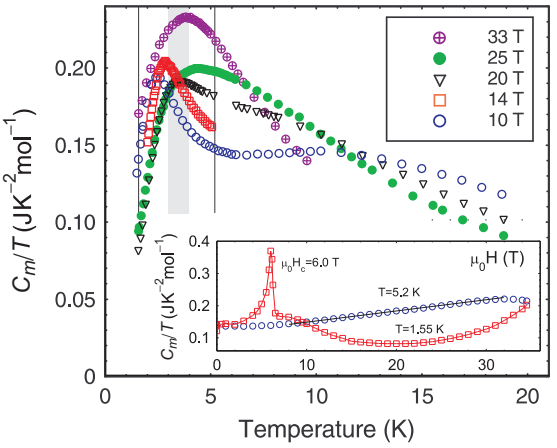

FIG. 3. (Color online) Magnetic part of the specific heat divided by temperature as a function of T measured at various magnetic fields using a high-field setup; the shadowed area corresponds to the formation of static 2D magnetic correlations as observed in an NMR experiment Ref. [14], and vertical lines mark temperatures of scans in the magnetic field shown in the inset. The solid line in the inset is a linear fit to data at $T = 5.2$ K in the intermediate-field range.

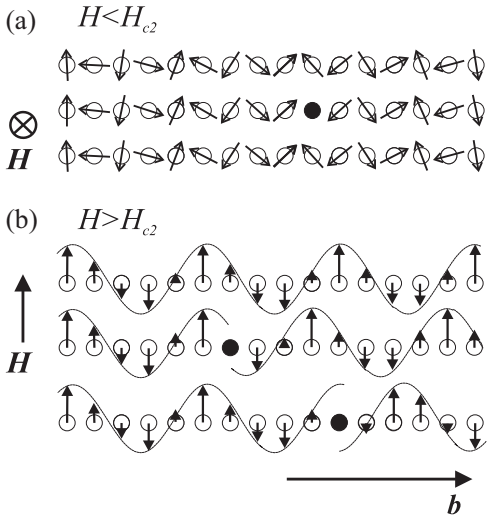

FIG. 4. Schematic of the influence of defects on (a) the spiral state and (b) the spin-modulated state at $\mu_0 H \simeq 20$ T. The defects are shown by black dots. The spiral state is nearly insensitive to the chain break whereas the phase of a spin-modulated chain is randomly shifted at the point of the defect.

A further increase in the applied magnetic field leads to a considerable change in the specific heat behavior (see Fig. 3). A broad hump in the C_m/T vs T curve preceding the formation of static 2D correlations shifts to somewhat higher temperatures, whereas the quasi-1D linear part (constant for C_m/T) breaks down at fields above 20 T. It is replaced by another broad feature merging with the first one at a maximum experimental field of 33 T. Two scans in an applied magnetic field performed at constant temperature below (1.55 K) and above (5.2 K) the ordering transition $T_N = 2.27$ K at ($H = 0$) are presented in the inset to Fig. 3. The low-T curve has a sharp peak associated with the transition from a helical phase at $\mu_0 H_{c2} = 6.0$ T followed by a gradual decrease in magnitude towards higher fields. The specific heat reaches its minimum around 20 T and then starts to increase as the field enters the range of critical fluctuations near saturation. In contrast, the high-T curve demonstrates a crossover from a nearly constant to a linear field dependence $C/T(H)$ (the fit is shown by the solid line) extending to about 25 T. The final downturn of the specific heat developing at fields above 30 T indicates the approach of the system to the saturated state.

III. DISCUSSION

We will now discuss the specific heat data obtained for high-quality single-crystal samples of $LiCuVO_4$ at field and temperatures of spin-liquid and ordered helical and SM phases. The specific heat in the spin-liquid phase for temperatures of $5 \lesssim T \lesssim 10$ K is a nearly linear function of T at low fields ($H \lesssim H_{sat}/4$) and becomes nonlinear at higher fields. The observed evolution is in qualitative agreement with numerical results obtained for a Heisenberg $S = \frac{1}{2}$ chain model [22]. The temperature dependence of the specific heat in the ordered helical state can be roughly approximated as a sum of linear and $C_m \propto T^3$ terms whereas for the SM state the cubic term is replaced by the $C_m \propto T^2$ contribution. Different exponents in power laws point to 3D and quasi-2D properties, respectively, of these phases confirming that the antiferromagnetic ordering between neighboring ab planes in the SM structure is destroyed. This effect was previously reported in neutron-scattering and NMR measurements [16,23]. The replacement of a sharp λ anomaly at the transition to the helical state by a broad feature at the crossover to the SM state gives another hint of this change.

In the following we propose a qualitative model to explain this different dimensional behavior by considering the effect of a nonmagnetic impurity. A composition study of $LiCuVO_4$ reveals a Li deficiency of a few percent even in crystals grown using the low-temperature technique which provides crystals of the highest perfection. It was argued that the Li deficiency results in holes with spins $S = \frac{1}{2}$ localized on oxygen which in turn form a Zhang-Rice singlet with the neighboring copper spin [17,24]. Such a singlet should be equivalent to a nonmagnetic impurity replacing a Cu spin and will provoke an unusual magnetic state in its vicinity with the two nearest ferromagnetic exchange bonds removed but with a conserved antiferromagnetic bond between the two parts of the interrupted chain. The presence of such defects in $LiCuVO_4$ single crystals of the same series as in this paper was suggested in order to explain the bulk magnetization process as well as the vanadium NMR spectra in the vicinity of the saturation field [13]. A schematic of helical and SM spin chains broken by a nonmagnetic defect is shown in Fig. 4. In contrast to a spin chain with only a nearest-neighbor exchange interaction, the frustrated J_1-J_2 chain is not fully broken by a nonmagnetic impurity. The magnetic moments on both sides of the defect are coupled by indirect antiferromagnetic exchange interaction leading to a local distortion and phase shift of an incommensurate exchange structure.

Obviously, the presence of this type of defect does not significantly disturb the helical magnetic structure in

$LiCuVO_4$ since the incommensurate wave vector of the helix $k_{ic} = 0.468 \times 2\pi/b$ (the unit cell of $LiCuVO_4$ contains two magnetic ions of Cu) corresponds to the angle between next-nearest-neighbor spins close to π [see Fig. 4(a)] and does not depend on the applied field. A residual phase shift of a helical structure near the defect may be eliminated due to an intrachain exchange interaction so that the initial 3D long-range ordering is not suppressed. In contrast, the influence of defects on the SM ordering is expected to be more pronounced for the following reasons. The wave vector of a SM structure in a 1D J_1-J_2 model is field dependent and expressed as follows: $k_{ic} = [1 - M(H)/M_{sat}]\pi/b$ [1,3–6]. This relation has been traced experimentally in the field range below 15 T (Refs. [16,25]), and therefore, the value k_{ic} is significantly less than π/b at all fields above H_{c2}. The elongation of the spin-modulation period along the chain in the field leads to a random shift of its phase at each defect [see Fig. 4(b), the scheme of the moment distribution over the chain is presented for $\mu_0 H \simeq 20$ T]. The boundary conditions for spins at both ends of a finite chain should depend on its length leading to an uncertainty in the phase shift of an incommensurate structure due to a random distribution of the vacancies. As in the case of a helical structure, the effect of intrachain exchange interactions is to restore these broken correlations and establish a 3D ordering. Taking into account the hierarchy of exchange parameters (the interaction between c planes is the smallest one) correlations between spins in neighboring ab planes are hindered, and the system remains in an effectively 2D ordered state. A similar suppression of 3D ordering was observed in the quasi-2D helical systems $LiCu_2O_2$ and $CuCrO_2$ doped with nonmagnetic impurities [26,27]. Our scenario, implying the arbitrary phase shift of the incommensurate structure at the defect was also considered for $LiCu_2O_2$. The main differences of our model are in: (i) the quasi-1D nature of the spin system in $LiCuVO_4$ which amplifies the distortions due to random phase shifts and (ii) the peculiar wave-vector value of a helical structure (close to $\pi/2$) which leaves it nearly undisturbed by impurities whereas an incommensurate SM structure is strongly influenced by defects.

IV. CONCLUSIONS

In conclusion, a specific heat experiment was performed on high-quality single crystals of $LiCuVO_4$. The results show that although a helical spin state observed in the low-field range $H < H_{c2}$ clearly demonstrates 3D magnetic ordering, the field-induced magnetic phase at $H > H_{c2}$ has properties peculiar to a quasi-2D system. We propose a simple model to describe how nonmagnetic defects in the Cu^{2+} chains can destroy 3D long-range ordering in a SM phase but leave it undisturbed in the helical phase. In addition, the proposed model allows one to simultaneously explain the results of both NMR (Refs. [13–15]) and neutron-scattering measurements (Ref. [16]) resolving the existing discrepancy in their interpretations. According to NMR data, the magnetic phases at both sides of H_{c2} are dipolar so that the average values of the magnetic moments of the Cu ions are nonzero on the timescale of the NMR experiment (~ 0.1 s in T_1 time-relaxation measurements). This proves the presence of static magnetic correlations and precludes an identification of the spin-nematic state, assumed in Ref. [16] for higher magnetic fields $H > H_{c2}$. Nevertheless, the short-range character of these correlations especially in the direction perpendicular to the ab planes detected in neutron-diffraction patterns can be understood using the above model describing the suppression of a 3D long-range order by nonmagnetic defects. Further specific heat experiments extending to the vicinity of the saturation field (about 45 T) are especially interesting in the prospect of possible observation of the transition from a SM into a theoretically predicted quadrupole nematic state.

ACKNOWLEDGMENTS

This work was supported by Grant No. 13-02-00637 of the Russian Fund for Basic Research, Program of Russian Scientific Schools, and by the German Research Society (DFG) via TRR80. A portion of this work was performed at the National High Magnetic Field Laboratory, which is supported by National Science Foundation Cooperative Agreement No. DMR-1157490 and the State of Florida. The authors thank M. Zhitomirsky for stimulating discussions.

[1] T. Hikihara, L. Kecke, T. Momoi, and A. Furusaki, Phys. Rev. B **78**, 144404 (2008).
[2] S. Nishimoto, S.-L. Drechsler, R. Kuzian *et al.*, Europhys. Lett. **98**, 37007 (2012).
[3] O. A. Starykh and L. Balents, Phys. Rev. B **89**, 104407 (2014).
[4] L. Kecke, T. Momoi, and A. Furusaki, Phys. Rev. B **76**, 060407(R) (2007).
[5] J. Sudan, A. Lüscher, and A. M. Läuchli, Phys. Rev. B **80**, 140402(R) (2009).
[6] M. Sato, T. Momoi, and A. Furusaki, Phys. Rev. B **79**, 060406(R) (2009).
[7] M. E. Zhitomirsky and H. Tsunetsugu, Europhys. Lett. **92**, 37001 (2010).
[8] B. J. Gibson, R. K. Kremer, A. V. Prokofiev *et al.*, Physica B **350**, e253 (2004).
[9] M. Enderle, C. Mukherjee, B. Fåk *et al.*, Europhys. Lett. **70**, 237 (2005).
[10] F. Heidrich-Meisner, I. P. McCulloch, and A. K. Kolezhuk, Phys. Rev. B **80**, 144417 (2009).
[11] L. E. Svistov, T. Fujita, H. Yamaguchi *et al.*, JETP Lett. **93**, 21 (2011).
[12] A. V. Chubukov, Phys. Rev. B **44**, 4693 (1991).
[13] N. Büttgen, K. Nawa, T. Fujita, M. Hagiwara, P. Kuhns, A. Prokofiev, A. P. Reyes, L. E. Svistov, K. Yoshimura, and M. Takigawa, Phys. Rev. B **90**, 134401 (2014).
[14] N. Büttgen, P. Kuhns, A. Prokofiev, A. P. Reyes, and L. E. Svistov, Phys. Rev. B **85**, 214421 (2012).
[15] K. Nawa, M. Takigawa, M. Yoshida, and K. Yoshimura, J. Phys. Soc. Jpn. **82**, 094709 (2013).
[16] M. Mourigal, M. Enderle, B. Fåk, R. K. Kremer, J. M. Law, A. Schneidewind, A. Hiess, and A. Prokofiev, Phys. Rev. Lett. **109**, 027203 (2012).
[17] A. V. Prokofiev, I. G. Vasilyeva, V. N. Ikorskii *et al.*, Solid State Chem. **177**, 3131 (2004).

[18] J. Sirker, Phys. Rev. B **81**, 014419 (2010).
[19] M. Yamaguchi, T. Furuta, and M. Ishikawa, J. Phys. Soc. Jpn. **65**, 2998 (1996).
[20] I. A. Smirnov, D. Wlosewicz, A. V. Prokofiev, and W. Assmus, Phys. Solid State **46**, 1933 (2004).
[21] M. G. Banks, F. Heidrich-Meisner, A. Honecker, H. Rakoto, J.-M. Broto, and R. K. Kremer, J. Phys.: Condens. Matter **19**, 145227 (2007).
[22] A. Klümper, Eur. Phys. J. B **5**, 677 (1998).
[23] N. Büttgen, W. Kraetschmer, L. E. Svistov, L. A. Prozorova, and A. Prokofiev, Phys. Rev. B **81**, 052403 (2010).
[24] F. C. Zhang and T. M. Rice, Phys. Rev. B **37**, 3759 (1988).
[25] T. Masuda, M. Hagihala, Y. Kondoh *et al.*, J. Phys. Soc. Jpn. **80**, 113705 (2011).
[26] A. A. Bush, N. Büttgen, A. A. Gippius, V. N. Glazkov, W. Kraetschmer, L. A. Prozorova, L. E. Svistov, A. M. Vasiliev, and A. Zheludev, Phys. Rev. B **88**, 104411 (2013).
[27] R. Kajimoto, K. Nakajima, S. Ohira-Kawamura *et al.*, J. Phys. Soc. Jpn. **82**, 054702 (2013).